Inorg. Chem. **2004**, *43*, 3656–3662

$[Mn_2(AsS_4)_4]^{8-}$ and $[Cd_2(AsS_4)_2(AsS_5)_2]^{8-}$: Discrete Clusters with High Negative Charge from Alkali Metal Polythioarsenate Fluxes

Ratnasabapathy G. Iyer and Mercouri G. Kanatzidis*

Department of Chemistry, Michigan State University, East Lansing, Michigan 48824

Received January 23, 2004

The reaction of Mn and Cd in alkali metal polythioarsenate fluxes afforded four new compounds featuring molecular anions. $K_8[Mn_2(AsS_4)_4]$ (**I**) crystallizes in the monoclinic space group $P2/n$ with $a = 9.1818(8)$ Å, $b = 8.5867(8)$ Å, $c = 20.3802(19)$ Å, and $\beta = 95.095(2)°$. $Rb_8[Mn_2(AsS_4)_4]$ (**II**) and $Cs_8[Mn_2(AsS_4)_4]$ (**III**) both crystallize in the triclinic space group $P\bar{1}$ with $a = 9.079(3)$ Å, $b = 9.197(3)$ Å, $c = 11.219(4)$ Å, $\alpha = 105.958(7)°$, $\beta = 103.950(5)°$, and $\gamma = 92.612(6)°$ for **II** and $a = 9.420(5)$ Å, $b = 9.559(5)$ Å, $c = 11.496(7)$ Å, $\alpha = 105.606(14)°$, $\beta = 102.999(12)°$, and $\gamma = 92.423(14)°$ for **III**. The discrete dimeric $[Mn_2(AsS_4)_4]^{8-}$ clusters in these compounds are composed of two octahedral Mn^{2+} ions bridged by two $[AsS_4]^{3-}$ units and chelated each by a $[AsS_4]^{3-}$ unit. $Rb_8[Cd_2(AsS_4)_2(AsS_5)_2]$ (**IV**) crystallizes in $P\bar{1}$ with $a = 9.122(2)$ Å, $b = 9.285(2)$ Å, $c = 12.400(3)$ Å, $\alpha = 111.700(6)°$, $\beta = 108.744°$, and $\gamma = 90.163(5)°$. Owing to the greater size of Cd compared to Mn, the Cd centers in this compound are bridged by $[AsS_5]^{3-}$ units. The $[Cd_2(AsS_4)_4]^{8-}$ cluster is a minor component cocrystallized in the lattice. These compounds are yellow in color and soluble in water.

Introduction

Traditionally "all-inorganic" chalcogenide cluster compounds have been prepared in solution near room temperature using standard precipitation techniques and aided by the use of organic counterions.[1] Inorganic clusters have often been thought of as thermally too sensitive to be stable at high temperatures, and highly charged clusters have been exceedingly difficult to deal with in water or organic solvents. The development of low-temperature techniques including the solventothermal method and the molten alkali metal flux method has made it easier to isolate compounds with discrete clusters. Although primarily designed for extended solids, the molten alkali metal polychalcogenide flux method[2] can be a promising synthetic technique for molecular chalcogenides as well. For example, alkali metal polychalcophosphate fluxes have yielded several such compounds including $K_6[Cr_2(PS_4)_4]$,[3] $Rb_8[M_4(Se_2)_2(PSe_4)_4]$ (M = Cd, Hg),[4] $Cs_5[In(P_2Se_6)_2]$,[5] $K_9[Ce(PS_4)_4]$,[6] $Rb_9[Ce(PSe_4)_4]$,[7] $A_5[Sn(PSe_5)_3]$ (A = K, Rb),[8] $A_6[Sn_2Se_4(PSe_5)_2]$ (A = Rb, Cs),[8] $A_5[An(PS_4)_3]$ (A = K, Rb, Cs; An = U, Th),[9] $Cs_{10}[Pd(PSe_4)_4]$,[10] $K_4[Pd(PS_4)_2]$,[10] and $Cs_4[Pd(PSe_4)_2]$.[10] Molecular salts are best obtained under highly basic flux conditions.[2] It is noteworthy that access to these highly charged anions would be extremely difficult using "wet" chemistry.

Since the broad synthetic scope of polychalcophosphate fluxes[11] in discovering new materials has been established, we decided to investigate how the corresponding chalcoarsenate fluxes might behave. Our initial experiments with main group metals, in alkali metal thioarsenate flux yielded us $Cs_2SnAs_2Q_9$ (Q = S, Se)[12] and $A_6[InAs_3S_{13}]$[13] (A = K, Cs), which contain discrete molecular complexes of $[Sn(AsS_4)(AsS_5)]^{2-}$ and $[In(AsS_4)_2(AsS_5)]^{6-}$, respectively.

* Author to whom correspondence should be addressed. E-mail: kanatzid@cem.msu.edu.

(1) (a) Kanatzidis, M. G.; Huang, S. P. *Coord. Chem. Rev.* **1994**, *130*, 509. (b) Chung, D. Y.; Huang, S. P.; Kim, K. W.; Kanatzidis, M. G. *Inorg. Chem.* **1995**, *34*, 4292. (c) Eichhorn, B. W.; Mattamana, S. P.; Gardner, D. R.; Fettinger, J. C. *J. Am. Chem. Soc.* **1998**, *120*, 9708. (d) Bollinger, J. C.; Ibers, J. A. *Inorg. Chem.* **1995**, *34*, 1859. (e) Wang, C.; Haushalter, R. C. *Inorg. Chim. Acta* **1999**, *288*, 1.
(2) Sutorik, A. C.; Kanatzidis, M. G. *Prog. Inorg. Chem.* **1995**, *43*, 151.
(3) Derstroff, V.; Kwenofontov, V.; Gutlich, P.; Tremel, W. *Chem. Commun.* **1998**, 187.
(4) Choundroudis, K.; Kanatzidis, M. G. *Chem. Commun.* **1997**, 401.
(5) Chondroudis, K.; Chakrabarty, D.; Axtell, E. A.; Kanatzidis, M. G. *Z. Anorg. Allg. Chem.* **1998**, *624*, 975.
(6) Gauthier, G.; Jobic, S.; Danaire, V.; Brec, R.; Evain, M. *Acta Crystallogr.* **2000**, *C56*, 117.
(7) Chondroudis, K.; Kanatzidis, M. G. *Inorg. Chem. Commun.* **1998**, 55.
(8) Chondroudis, K.; Kanatzidis, M. G. *Chem. Commun.* **1996**, 1371.
(9) Hess, R.; Abney, K. D.; Burris, J. L.; Hochheimer, H. D.; Dorhout, P. K. *Inorg. Chem.* **2001**, *40*, 2851.
(10) Chondroudis, K.; Kanatzidis, M. G.; Sayettat, J.; Jobic, S.; Brec, R. *Inorg. Chem.* **1997**, *36*, 5859.
(11) Kanatzidis, M. G. *Curr. Opin. Solid State Mater. Sci.* **1997**, *2*, 139.
(12) Iyer, R. G.; Do, J.; Kanatzidis, M. G. *Inorg. Chem.* **2003**, *42*, 1475.
(13) Iyer, R. G.; Kanatzidis, M. G. Manuscript in preparation.

10.1021/ic049905u CCC: $27.50
Published on Web 05/18/2004

We report here that the reactivity of Mn and Cd in alkali metal polythioarsenate fluxes (i.e. molten $AAsS_x$ (A = alkali metal)) affords salts containing the highly charged molecular thioarsenate complexes $[Mn_2(AsS_4)_4]^{8-}$ and $[Cd_2(AsS_4)_2(AsS_5)_2]^{8-}$. It is interesting that these salts are subsequently soluble in water. In addition, the cadmium complex presents a rare example of a sulfur-coordinated Cd^{2+} center with a full octahedral geometry.

Experimental Section

The following reagents were used as obtained: Rb, Cs metals (analytical reagent, Johnson Matthey/AESAR Group, Seabrook, NH); K metal (analytical reagent, Aldrich Chemical Co., Milwaukee, WI); S (99.9%, Strem Chemicals, Newburyport, MA); Cd, Mn (Johnson Matthey/AESAR Group, Seabrook, NH); As_2S_3 (99.9%; Strem Chemicals, Newburyport, MA). K_2S, Rb_2S, and Cs_2S were made by the reaction of the alkali metal and sulfur in liquid ammonia using a modified literature procedure.[14]

Synthesis. $K_8[Mn_2(AsS_4)_4]$ (I) was prepared by reacting a mixture of K_2S (0.055 g, 0.5 mmol), Mn (0.014 g, 0.25 mmol), As_2S_3 (0.062 g, 0.25 mmol), and S (0.08 g, 2.5 mmol) in the ratio 2:1:1:10. All manipulations were done in a glovebox under nitrogen atmosphere. The reactants were loaded in fused silica tube and sealed under vacuum ($<10^{-4}$ Torr). The tube was then inserted in a furnace and heated to 500 °C in 10 h. It was isothermed at this temperature for 60 h before cooling down to 250 °C at the rate of 5 °C/h, followed by rapid quenching to room temperature. Isolation of the product using N_2-bubbled *N*,*N*-dimethylformamide revealed large golden yellow crystals (~70% yield based on Mn) and green microcrystals. Energy dispersive spectroscopy revealed an average composition of "$K_{6.4}Mn_3As_4S_{14.4}$" and "$K_2Mn_{2.3}AsS_{4.7}$" for the golden yellow crystals and the green microcrystals, respectively. The powder diffraction pattern of the yellow crystals compared very well to the simulated pattern obtained from single-crystal refinement.

$Rb_8[Mn_2(AsS_4)_4]$ (II) was synthesized from a $Rb_2S/Mn/As_2S_3/S$ ratio of 3:1:1:10 using the same heating profile as above. The product consisted of bright yellow, colorless, and black crystals. Electron microscopy analysis on several of the yellow crystals gave an average composition of "$Rb_{10.2}Mn_2As_4S_{13.6}$". The colorless and the black crystals were Rb_3AsS_4 and MnS, respectively.

$Cs_8[Mn_2(AsS_4)_4]$ (III) was obtained from a reaction of $Cs_2S/Mn/As_2S_3/S$ in the ratio 2:1:1:10. The method used was identical with mentioned above, and the product consisted of yellow, colorless, and black crystals. Elemental analysis using EDS on the yellow crystals confirmed the presence of all four elements with an average composition of "$Cs_{7.9}Mn_{1.5}As_{4.3}S_{15.9}$".

$Rb_8[Cd_2(AsS_4)_2(AsS_5)_2]$ (IV) was the product of the reaction of $Rb_2S/Cd/As_2S_3/S$ in the ratio 2:1:1:10. The synthetic conditions remained the same as above and along with the title compound were obtained colorless crystals of Rb_3AsS_4 and Rb_2S. The impurities were a minor part of the product as determined from powder diffraction pattern. EDS measurements on the yellow crystals gave an average value of "$Rb_{9.6}Cd_2As_{4.6}S_{19.6}$".

Physical Measurements. (a) Powder X-ray Diffraction. A calibrated CPS 120 INEL X-ray powder diffractometer equipped with a position-sensitive detector, operating at 40 kV/25 mA with a flat geometry and employing Cu Kα radiation, was used to obtain diffractograms. Observed powder patterns were compared with powder patterns calculated using the Cerius[2] software package.

(b) Energy-Dispersive Spectroscopy. Energy-dispersive spectroscopy (EDS), to analyze the composition of the compounds, was done on a JEOL 6400V scanning electron microscope (SEM) equipped with a NORAN detector. Data were acquired with an accelerating voltage of 20 kV and accumulation time of 45 s.

(c) UV/Vis/Near-IR and Infrared Spectroscopy. Optical diffuse reflectance measurements were made at room temperature using a Shimadzu UV-3101 PC double-beam, double-monochromator spectrophotometer operating in the 200−2500 nm region using a procedure described elsewhere in detail.[15]

FT-IR spectra were recorded as solids in a CsI matrix. The samples were ground with dry CsI into a fine powder and pressed into translucent pellets. The spectra were recorded in the far-IR region (600−100 cm^{-1}, 4 cm^{-1} resolution) using a Nicolet 740 FT-IR spectrometer equipped with a TGS/PE detector and a silicon beam splitter.

(d) Magnetic Susceptibility Measurements. Magnetization measurements as a function of applied magnetic field and temperature were made on a MPMS Quantum Design SQUID susceptometer in the temperature range of 2−300 K and magnetic fields of 0 to ±55 kG. The samples consisted of a few (5 or 6) large single crystals.

(e) Differential Thermal Analysis. Thermal studies were performed on Shimadzu DTA-50 thermal analyzer. Typically samples were heated to 600 °C at the rate of 10 °C/min and held there for 1 min, followed by cooling to 100 °C at the rate of −10 °C/ min. Residues of the DTA experiments were examined by powder X-ray diffraction. Multiple heating/cooling cycles were run to ascertain the reproducibility of the results.

(f) Single-Crystal X-ray Crystallography. A Bruker SMART Platform CCD diffractometer, operating at 50 kV/40 mA and employing graphite-monochromatized Mo Kα radiation was used to collect crystal diffraction data. A full sphere of data was collected for all compounds with scan widths of 0.3° in ω and an exposure time of at least 30 s/frame. Data were collected using the SMART program and integrated with the program SAINT using the orientation matrix obtained from SMART. An empirical absorption correction was done with the program SADABS, and all refinements were carried out with the SHELXTL[16] package of crystallographic programs. On the basis of systematic absences and intensity statistics, the space group was determined to be $P2/n$ for **I** and $P\bar{1}$ for **II**−**IV**. Refinement of **I**−**III** was straightforward to give final R1/wR2 values of 1.88/4.39, 2.27/5.41, and 4.28/12.24, respectively. For **IV**, after the initial round of least squares, one Cd, four Rb, two As, and nine S atoms were found with R1/wR2 = 8.85/20.66. At this point, a high electron density peak (assigned As22) was observed at a distance of 0.72 Å from As2. Two more peaks, one close to the disulfide arm at 0.72 Å from S7 and 1.65 Å from S3 (assigned S10) and one 1.22 Å away from S9 (assigned S99), were observed. S10 and S99 were respectively 2.09 and 2.13 Å away from As22. Therefore, a disordered model was considered and structure refinement led to an occupancy of 85% for the $[AsS_5]^{3-}$ ligand and 15% for the $[AsS_4]^{3-}$ ligand. Anisotropic refinement gave final R1/wR2 values of 5.01/11.19. Crystallographic refinement details for all compounds are given in Table 1. Fractional atomic coordinates and anisotropic temperature factors are deposited

(14) Feher, F. In *Handbook of Preparative Inorganic Chemistry*; Brauer, G., Ed.; Ferdinand Enke: Stuttgart, Germany, 1954; Vol. 1, pp 280−281.

(15) Aitken, J. A.; Chondroudis, K.; Young, V. G.; Kanatzidis, M. G. *Inorg. Chem.* **2000**, *39*, 1525.

(16) *SMART, SAINT, SHELXTL: Data Collection and Processing Software for the SMART-CCD system*; Siemens Analytical X-ray Instruments Inc.: Madison, WI, 1997.

Table 1. Crystallographic Refinement Details of $K_8Mn_2As_4S_{16}$, $Rb_8Mn_2As_4S_{16}$, $Cs_8Mn_2As_4S_{16}$, and $Rb_8Cd_2As_4S_{18}$

param	$K_8Mn_2As_4S_{16}$	$Rb_8Mn_2As_4S_{16}$	$Cs_8Mn_2As_4S_{16}$	$Rb_8Cd_2As_4S_{18}$
space group	$P2/n$	$P\bar{1}$	$P\bar{1}$	$P\bar{1}$
a, Å	9.1818 (8)	9.079 (3)	9.420 (5)	9.122 (2)
b, Å	8.5867 (8)	9.197 (3)	9.559 (5)	9.285 (2)
c, Å	20.3802 (19)	11.219 (4)	11.496 (7)	12.400 (3)
α, deg	90	105.958 (7)	105.606 (14)	111.700 (6)
β, deg	95.095(2)	103.950 (5)	102.999 (12)	108.744 (5)
γ, deg	90	92.612 (6)	92.423 (14)	90.163 (5)
Z, V	4, 1600.5(3)	2, 867.8 (5)	2, 965.5 (9)	2, 915.2 (4)
D, mg/m^3	2.563	3.074	3.415	3.239
temp, K	173	293	293	173
λ, Å	0.710 73	0.710 73	0.710 73	0.710 73
μ, mm^{-1}	6.977	16.620	12.353	16.349
F(000)	1180	734	878	812
θ_{max}, deg	28.29	28.24	27.88	28.30
tot. reflns	16 097	8668	9201	9225
tot. unique reflns	3900	3921	4210	4291
no. params	137	145	136	173
refinement method	full-matrix least squares on F^2			
final R indices($I > 2\sigma(I)$)	R1[a] = 0.0188, wR2[b] = 0.0439	R1 = 0.0227, wR2 = 0.0541	R1 = 0.0428, wR2 = 0.1224	R1 = 0.0501, wR2 = 0.1119
R indices (all data)	R1 = 0.0218, wR2 = 0.0447	R1 = 0.0298, wR2 = 0.558	R1 = 0.0475, wR2 = 0.1254	R1 = 0.0666, wR2 = 0.1187
goodness of fit on F^2	1.039	1.000	1.053	1.042

[a] $R1 = \sum||F_o| - |F_c||/\sum|F_o|$. [b] $wR2 = \{\sum[w(F_o^2 - F_c^2)^2]/\sum[w(F_o^2)^2]\}^{1/2}$.

Table 2. Selected Bond Distances for $K_8Mn_2As_4S_{16}$ and $Rb_8Cd_2As_4S_{18}$

			$K_8Mn_2As_4S_{16}$		
As(1)−S(8)	2.1306(6)	K(1)−S(2)	3.3272(7)	K(3)−S(6)	3.3263(8)
As(1)−S(1)	2.1626(5)	K(1)−S(2)	3.5447(8)	K(3)−S(7)	3.5654(8)
As(1)−S(4)	2.1715(6)	K(1)−S(3)	3.1142(8)	K(3)−S(8)	3.3175(8)
As(1)−S(7)	2.1984(5)	K(1)−S(4)	3.4509(7)	K(4)−S(1)	3.2697(8)
As(2)−S(3)	2.1378(6)	K(1)−S(5)	3.1515(8)	K(4)−S(1)	3.2883(7)
As(2)−S(5)	2.1443(6)	K(1)−S(7)	3.3381(7)	K(4)−S(2)	3.3613(7)
As(2)−S(2)	2.1793(5)	K(1)−S(8)	3.3526(8)	K(4)−S(4)	3.2210(7)
As(2)−S(6)	2.1936(6)	K(1)−S(8)	3.4300(8)	K(4)−S(5)	3.2417(8)
Mn(1)−S(1)	2.5812(6)	K(1)−As(1)	3.6755(6)	K(4)−S(5)	3.1292(8)
Mn(1)−S(2)	2.5920(6)	K(2)−S(4)	2 × 3.5346(7)	K(4)−S(6)	3.4158(7)
Mn(1)−S(4)	2.6238(6)	K(2)−S(6)	2 × 3.3112(8)	K(4)−S(7)	3.7104(7)
Mn(1)−S(6)	2.6635(6)	K(2)−S(8)	2 × 3.2489(7)	K(4)−As(2)	3.6785(6)
Mn(1)−S(7)	2.7591(6)	K(3)−S(1)	3.5442(7)	K(5)−S(3)	2 × 3.1385(7)
Mn(1)−S(7)	2.7739(6)	K(3)−S(3)	3.1167(7)	K(5)−S(4)	2 × 3.1828(7)
Mn(1)− Mn(1)	4.070(1)	K(3)−S(3)	3.5402(8)	K(5)−S(6)	2 × 3.2566(7)
		K(3)−S(5)	3.1548(8)	K(5)−As(2)	3.7765(5)
			$Rb_8Cd_2As_4S_{18}$		
As(1)−S(1)	2.143(2)	Rb(1)−S(2)	3.599(2)	Rb(3)−S(1)	3.382(2)
As(1)−S(5)	2.152(2)	Rb(1)−S(4)	3.479(2)	Rb(3)−S(1)	3.667(2)
As(1)−S(2)	2.177(2)	Rb(1)−S(5)	3.359(2)	Rb(3)−S(3)	3.650(3)
As(1)−S(4)	2.183(2)	Rb(1)−S(5)	3.309(2)	Rb(3)−S(4)	3.705(2)
As(2)−As(22)	0.536(13)	Rb(1)−S(6)	3.380(2)	Rb(3)−S(4)	3.458(2)
As(2)−S(99)	1.79(2)	Rb(1)−S(6)	3.634(3)	Rb(3)−S(5)	3.688(2)
As(2)−S(9)	2.111(3)	Rb(1)−S(7)	3.428(4)	Rb(3)−S(8)	3.482(2)
As(2)−S(8)	2.130(3)	Rb(1)−S(8)	3.324(2)	Rb(3)−S(9)	3.606(3)
As(2)−S(6)	2.174(3)	Rb(1)−As(1)	3.8262(12)	Rb(3)−S(9)	3.471(3)
As(2)−S(3)	2.250(3)	Rb(1)−As(2)	4.031(2)	Rb(3)−S(99)	3.64(2)
As(22)−S(6)	1.956(11)	Rb(1)−As(22)	4.065(11)	Rb(3)−As(1)	3.6801(13)
As(22)−S(3)	2.023(12)	Rb(2)−S(1)	3.397(2)	Rb(3)−As(2)	3.733(2)
As(22)−S(99)	2.11(2)	Rb(2)−S(2)	3.379(2)	Rb(4)−S(1)	3.259(2)
As(22)−S(8)	2.210(10)	Rb(2)−S(2)	3.489(2)	Rb(4)−S(1)	3.722(2)
As(22)−S(10)	2.27(3)	Rb(2)−S(3)	3.235(2)	Rb(4)−S(3)	3.537(3)
Cd(1)−S(10)	2.70(2)	Rb(2)−S(5)	3.317(2)	Rb(4)−S(4)	3.455(2)
Cd(1)−S(8)	2.705(2)	Rb(2)−S(6)	3.727(3)	Rb(4)−S(5)	3.335(2)
Cd(1)−S(2)	2.711(2)	Rb(2)−S(7)	3.836(3)	Rb(4)−S(6)	3.550(2)
Cd(1)−S(4)	2.716(2)	Rb(2)−S(8)	3.319(2)	Rb(4)−S(7)	3.634(4)
Cd(1)−S(7)	2.720(3)	Rb(2)−S(9)	3.453(3)	Rb(4)−S(9)	3.389(3)
Cd(1)−S(6)	2.732(2)	Rb(2)−S(99)	3.72(2)	Rb(4)−S(99)	3.68(3)
Cd(1)−S(10)	2.811(19)	Rb(2)−S(99)	3.84(2)	Rb(4)−S(10)	3.91(2)
Cd(1)−S(7)	2.819(3)	Rb(2)−S(10)	3.51(2)	Rb(4)−As(2)	4.123(2)
Cd(1)−Cd(1)	3.960(1)				

in the Supporting Information. Selected distances and angles are given in Tables 2 and 3 for $K_8[Mn_2(AsS_4)_4]$ and $Rb_8[Cd_2(AsS_4)_2(AsS_5)_2]$.

Results and Discussion

Synthesis. The synthesis of $K_8[Mn_2(AsS_4)_4]$ was achieved by reaction of a mixture of a 2:1:1:10 ratio of K_2S/Mn/As_2S_3/S at 500 °C. The compound forms as large golden yellow crystals. The product was contaminated with green microcrystals of another quaternary phase of approximate composition "$K_2Mn_{2.3}AsS_{4.7}$" (based on EDS). The reaction involved the oxidative dissolution of the metal in the basic melt and the subsequent coordination of the divalent metal cations with the present $[AsS_x]^{3-}$ anions. Reaction parameters

Table 3. Selected Bond Angles for $K_8Mn_2As_4S_{16}$ and $Rb_8Cd_2As_4S_{18}$

		$K_8Mn_2As_4S_{16}$			
S(8)−As(1)−S(1)	111.38(2)	S(3)−As(2)−S(6)	113.08(2)	S(1)−Mn(1)−S(7)	90.038(19)
S(8)−As(1)−S(4)	112.56(2)	S(5)−As(2)−S(6)	111.00(2)	S(2)−Mn(1)−S(7)	165.44(2)
S(1)−As(1)−S(4)	109.90(2)	S(2)−As(2)−S(6)	102.70(2)	S(4)−Mn(1)−S(7)	79.224(17)
S(8)−As(1)−S(7)	115.64(2)	S(1)−Mn(1)−S(2)	104.37(2)	S(6)−Mn(1)−S(7)	97.290(18)
S(1)−As(1)−S(7)	103.12(2)	S(1)−Mn(1)−S(4)	167.96(2)	S(1)−Mn(1)−S(7)	79.174(18)
S(4)−As(1)−S(7)	103.58(2)	S(2)−Mn(1)−S(4)	86.625(18)	S(2)−Mn(1)−S(7)	99.327(18)
S(3)−As(2)−S(5)	109.14(2)	S(1)−Mn(1)−S(6)	89.19(2)	S(4)−Mn(1)−S(7)	94.387(19)
S(3)−As(2)−S(2)	110.19(2)	S(2)−Mn(1)−S(6)	81.041(17)	S(6)−Mn(1)−S(7)	168.10(2)
S(5)−As(2)−S(2)	110.60(2)	S(4)−Mn(1)−S(6)	97.51(2)	S(7)−Mn(1)−S(7)	85.296(18)
		$Rb_8Cd_2As_4S_{18}$			
S(10)−Cd(1)−S(8)	94.1(5)	S(4)−Cd(1)−S(10)	92.9(4)	S(8)−As(2)−S(6)	111.76(13)
S(10)−Cd(1)−S(2)	103.7(4)	S(6)−Cd(1)−S(10)	101.1(4)	S(99)−As(2)−S(3)	74.0(9)
S(8)−Cd(1)−S(2)	85.00(6)	S(8)−Cd(1)−S(7)	81.37(9)	S(9)−As(2)−S(3)	103.67(13)
S(10)−Cd(1)−S(4)	169.5(5)	S(2)−Cd(1)−S(7)	102.93(8)	S(8)−As(2)−S(3)	104.73(11)
S(8)−Cd(1)−S(4)	96.30(7)	S(4)−Cd(1)−S(7)	177.09(9)	S(6)−As(2)−S(3)	106.76(12)
S(2)−Cd(1)−S(4)	78.52(6)	S(7)−Cd(1)−S(7)	88.78(10)	S(6)−As(22)−S(99)	105.8(8)
S(10)−Cd(1)−S(7)	89.2(4)	S(6)−Cd(1)−S(7)	86.48(9)	S(3)−As(22)−S(99)	73.0(9)
S(8)−Cd(1)−S(7)	90.63(9)	S(10)−Cd(1)−S(7)	84.9(4)	S(6)−As(22)−S(8)	117.5(5)
S(2)−Cd(1)−S(7)	166.70(9)	S(1)−As(1)−S(5)	108.08(9)	S(3)−As(22)−S(8)	110.0(5)
S(4)−Cd(1)−S(7)	89.51(8)	S(1)−As(1)−S(2)	111.02(9)	S(99)−As(22)−S(8)	115.2(7)
S(10)−Cd(1)−S(6)	73.7(5)	S(5)−As(1)−S(2)	112.61(9)	S(6)−As(22)−S(10)	100.5(7)
S(8)−Cd(1)−S(6)	167.85(7)	S(1)−As(1)−S(4)	111.09(9)	S(99)−As(22)−S(10)	115.7(10)
S(2)−Cd(1)−S(6)	97.81(7)	S(5)−As(1)−S(4)	110.08(8)	S(8)−As(22)−S(10)	101.6(7)
S(4)−Cd(1)−S(6)	95.84(7)	S(2)−As(1)−S(4)	103.95(8)	S(6)−As(22)−S(9)	103.5(5)
S(7)−Cd(1)−S(6)	89.09(9)	S(99)−As(2)−S(8)	136.9(6)	S(3)−As(22)−S(9)	95.0(5)
S(10)−Cd(1)−S(10)	88.1(6)	S(9)−As(2)−S(8)	114.47(13)	S(8)−As(22)−S(9)	95.4(5)
S(8)−Cd(1)−S(10)	77.9(4)	S(99)−As(2)−S(6)	109.5(7)	S(10)−As(22)−S(9)	139.7(7)
S(2)−Cd(1)−S(10)	160.0(4)	S(9)−As(2)−S(6)	114.28(12)		

were varied through the addition of K_2S and As_2S_3. Increasing the basicity of the flux, by adding K_2S, led to the formation of K_3AsS_4 along with the title compound. Our attempts to obtain pure $Rb_8[Mn_2(AsS_4)_4]$ and $Cs_8[Mn_2(AsS_4)_4]$ were unsuccessful as the compounds always formed with some amount of A_3AsS_4 and MnS. This effect is more pronounced on increasing the flux basicity by adding more alkali metal sulfide. Increasing the fraction of As_2S_3 always led to glassy products. No other phases were detected in any of the reactions.

The reactivity of Zn in potassium and rubidium thioarsenate fluxes was also explored. Using the same reaction conditions as above, we obtained A_3AsS_4 and ZnS. Further work needs to be done to establish an optimal synthetic ratio for isolating Zn analogues of these clusters.

$Rb_8[Cd_2(AsS_4)_2(AsS_5)_2]$ was isolated from a reaction of Rb_2S/Cd/As_2S_3/S ratio of 2:1:1:10. This system was more prone to give Rb_3AsS_4 and CdS on increasing the basicity of the reaction (i.e. increasing the fraction of Rb_2S). As with the Mn chemistry above, increasing the fraction of As_2S_3 yielded glassy phases.

The cluster compounds reported here are soluble in water but insoluble in ethanol and DMF. The aqueous solution of the $A_8Mn_2As_4S_{16}$ is initially yellow-brown in color but rapidly becomes colorless. This discoloration is so rapid that no absorption is observed in the UV−vis spectrum. After about 1 h, the solution becomes milky. For the $Rb_8Cd_2As_4S_{18}$ compound, a yellow precipitate is observed after about 0.5 day. The powder pattern of this yellow precipitate shows that it is CdS. These observations indicate that the clusters do not remain intact in solution and precludes their formation by wet chemistry. The clusters were found to be stable in air for at least 1 month.

The thermal response of **I** and **II** was measured using a differential thermal analyzer. The data revealed that **I** and **II** melt incongruently at 480 and 520 °C, respectively. The powder X-ray diffraction pattern of the residue taken after DTA showed the presence of MnS and amorphous $K(Rb)_xAs_yS_z$ along with the parent compound.

Structure of $K_8[Mn_2(AsS_4)_4]$. The structure of $A_8[Mn_2(AsS_4)_4]$ contains the discrete molecular $[Mn_2(AsS_4)_4]^{8-}$ clusters and charge-compensating A^+ cations. We will discuss the structural details of $K_8[Mn_2(AsS_4)_4]$. The clusters are centrosymmetric and consist of octahedrally coordinated Mn^{2+} ions linked by tetrahedral $[AsS_4]^{3-}$ units (Figure 1). Each Mn center is connected to three $[AsS_4]^{3-}$ ligands, and each ligand uses two of its S atoms to bind the metal. There are two different kinds of $[AsS_4]^{3-}$ ligands, terminal and bridging. The terminal $[AsS_4]^{3-}$ ligand uses two of its sulfur arms to chelate to a single Mn atom. The bridging $[AsS_4]^{3-}$ ligand uses three of its sulfur atoms, two binding to two Mn atoms and the third S atom forming a bridge between the metals. The fourth S atom remains nonbonding. Alternatively, two MnS_6 octahedra edge share with four AsS_4 tetrahedra to form the binuclear cluster.

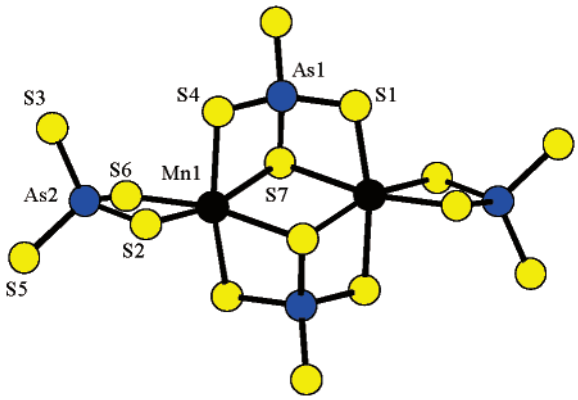

Figure 1. $[Mn_2(AsS_4)_4]^{8-}$ molecular anion with labeling. The dark circles are Mn, blue circles are As, and yellow circles are S.

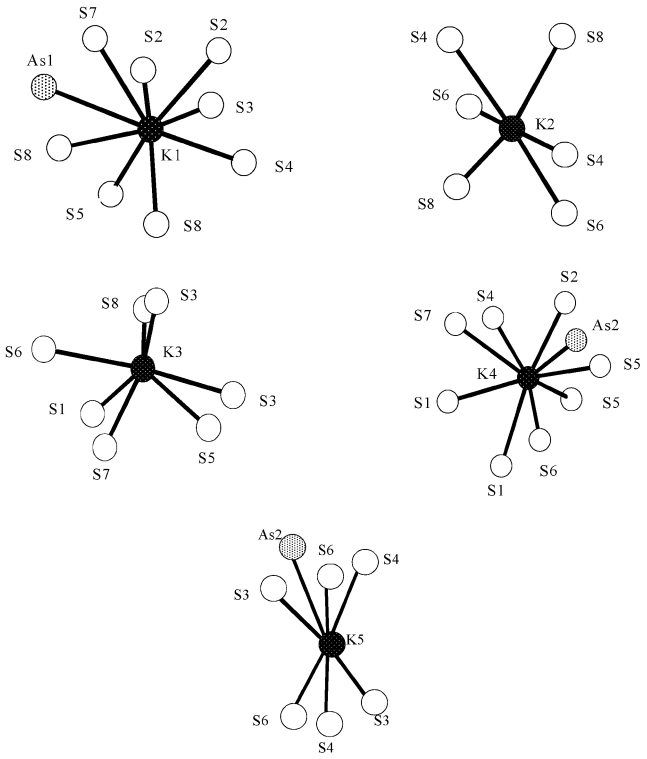

Figure 2. Coordination environments of the five crystallographically different K^+ cations in $K_8[Mn_2(AsS_4)_4]$.

The intracore Mn−Mn distance is 4.070(1) Å. Mn−S distances range from 2.5812(6) to 2.7739(6) Å (Table 2). As−S distances are normal between 2.1306(6) and 2.1984(5) Å for the terminal unit and between 2.1378(6) and 2.1936(6) Å for the bridging ligand. MnS_6 is a distorted octahedron with S−Mn−S bond angles varying from 79.174(18) to 167.96(2)°. The $[AsS_4]^{3-}$ tetrahedra are also distorted from ideal tetrahedral geometry with S−As−S bond angles between 103.12(2) and 115.64(2)° for bridging AsS_4 and between 102.70(2) and 113.08(2)° for the terminal ligand (Table 3).

There are 5 crystallographically unique K^+ ions. K1 sits in a nine coordinate pocket created by 8 S atoms and an As atom with distances between 3.1142(8) and 3.6755(6) Å. K2 is coordinated to 6 S atoms in the range 3.2489(7)−3.5346(7) Å. K3 is coordinated to 7 S atoms with bond distances ranging from 3.1167(7) to 3.5654(8) Å. K4 is connected to 8 S atoms and an As atom at distances 3.1292(8)−3.7104(7) Å. K5 is heptacoordinated by 6 S atoms and an As atom ranging from 3.1385(7) to 3.7765(5) Å. Figure 2 shows the coordination environments of the K cations.

In the case of the Rb and Cs analogues the structure of the core remains the same; however, the octahedral angles in the MnS_6 and AsS_4 groups are more distorted presumably due to the slightly different packing forces arising from the presence of the bigger alkali metals. This also leads to a lowering of symmetry in the overall structure from monoclinic $P2/n$ for $K_8Mn_2As_4S_{16}$ to $P\bar{1}$ for the Rb and Cs phases. Mn−Mn distance within the core increases to 4.176(1) and 4.327(1) Å for the Rb and Cs compounds, respectively.

Structure of $Rb_8(Cd_2(AsS_4)_2(AsS_5)_2$. The structure of $Rb_8(Cd_2(AsS_4)_2(AsS_5)_2$ presents an interesting case of ligand size adjustment to counter the size of the transition metal. The structure of this compound is similar to that of the Mn phase and consists of $[Cd_2(AsS_5)_2(AsS_4)_2]^{8-}$ clusters (Figure 3). The interesting aspect in this structure is the presence of the tetrahedral $[AsS_5]^{3-}$ ligand which is derived from the $[AsS_4]^{3-}$ tetrahedron by substituting a terminal S atom with a disulfide S_2^{2-} unit. The presence of the larger Cd^{2+} ion in place of a Mn^{2+} probably puts a strain on the bridging $[AsS_4]^{3-}$ ligand causing the system to release this strain by taking in an additional S atom from the flux to form $[AsS_5]^{3-}$ and the ensuing molecular $[Cd_2(AsS_5)_2(AsS_4)_2]^{8-}$ unit. Thus, this cluster is composed of two Cd atoms coordinated to two $[AsS_4]^{3-}$ units and bridged by two $[AsS_5]^{3-}$ units. This is by no means to say that $[Cd_2(AsS_4)_4]^{8-}$ does not exist. The refinement of this structure showed that the $[Cd_2(AsS_5)_2(AsS_4)_2]^{8-}$ anion is disordered with $[Cd_2(AsS_4)_4]^{8-}$ (15%) though the percentage of the former (85%) is much greater. Our attempts to isolate pure $Rb_8[Cd_2(AsS_4)_4]$ were however unsuccessful.

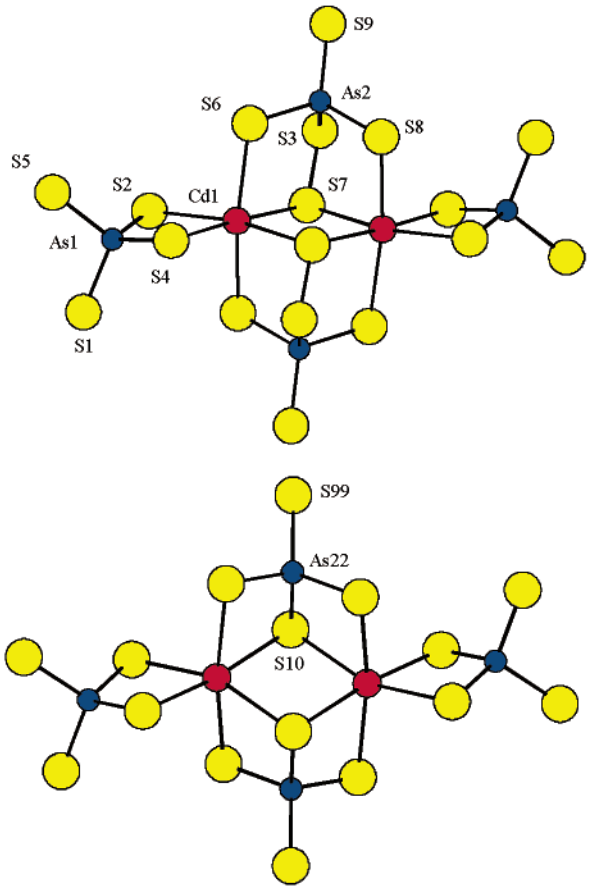

Figure 3. (a) Cluster anion $[Cd_2(AsS_4)_2(AsS_5)_2]^{8-}$ (major component) and (b) minor component $[Cd_2(AsS_4)_4]^{8-}$. Red circles are Cd, blue circles are As, and yellow circles are S.

The octahedral geometry of Cd^{2+} ions observed in $[Cd_2(AsS_5)_2(AsS_4)_2]^{8-}$ is indeed unusual for a sulfur-based coordination environment. In the vast majority of cases this metal ion prefers the standard tetrahedral geometry.[17]

In this structure, Cd−S bond distances range from 2.705(2) to 2.819(3) Å. As−S distances vary from 2.112(3) to 2.250(3) Å for AsS_5 and 2.143(2) to 2.183(2) Å for AsS_4 (Table 2). The S−S distance is normal at 2.071(4) Å. The

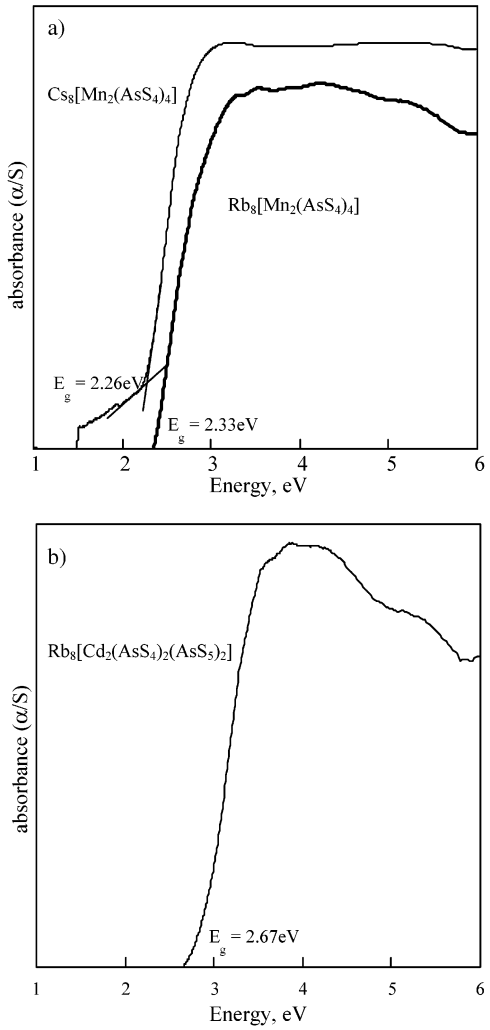

Figure 4. (a) Optical absorption spectra of $Cs_8[Mn_2(AsS_4)_4]$ and $Rb_8[Mn_2(AsS_4)_4]$ showing energy gaps at 2.26 and 2.33 eV, respectively. (b) Optical absorption spectra of $Rb_8[Cd_2(AsS_4)_2(AsS_5)_2]$ with an onset at 2.67 eV.

Cd−Cd distance within the core is 3.960(1) Å. The formation of the AsS_5 ligand reduces the distortion of the CdS_6 octahedra with S−Cd−S bond angles being closer to 90 and 180°. S−As−S bond angles are slightly distorted ranging from 103.95(8) to 112.61(9)° (Table 3).

The Mn and Cd clusters are reminiscent of the clusters encountered in $K_6Cr_2(PS_4)_4$,[3] which also consists of a binuclear Cr center that is bonded by 4 PS_4 units in a fashion identical with that described above. The one-dimensional compound $K_3Cr_2P_3S_{12}$[18] has the same core that shares edges with another core through the terminal PS_4 tetrahedron. It is interesting to note that $K_6Cr_2P_4S_{16}$ can be conceptually obtained from $K_3Cr_2P_3S_{12}$ by addition of 1 equiv of K_3PS_4. A dimeric core can be seen in $A_5An(PS_4)_3$ (An = U, Th).[8] However in these compounds, there are two terminal $[PS_4]^{3-}$ units/metal ion. This structural motif seems to be very stable

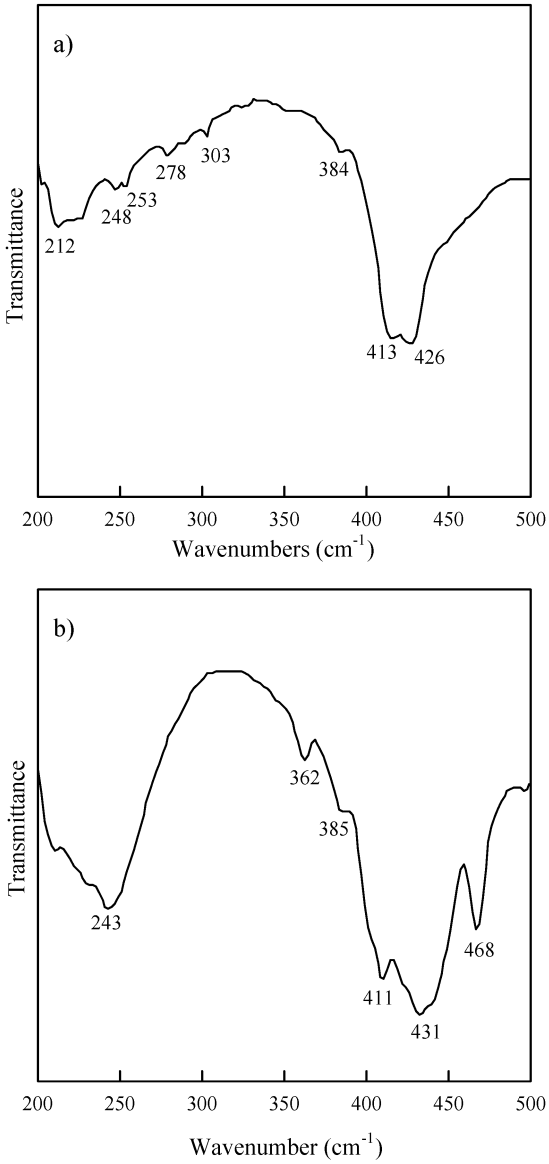

Figure 5. (a) Far IR spectrum of $K_8[Mn_2(AsS_4)_4]$ and (b) Far IR spectrum of $Rb_8[Cd_2(AsS_4)_2(AsS_5)_2]$. The peak at 468 cm^{-1} is attributed to S−S stretching.

and is observed in the chains of $A_3RE(PSe_4)_2$[19] and $K_3Pu(PS_4)_2$[20] and the layers of $Cs_3Bi_2(PS_4)_3$.[21]

Spectroscopy. Large crystals of $K_8[Mn_2(AsS_4)_4]$, $Rb_8[Mn_2(AsS_4)_4]$, $Cs_8[Mn_2(AsS_4)_4]$, and $Rb_8[Cd_2(AsS_4)_2(AsS_5)_2]$ were hand-picked and ground to powder for diffuse reflectance spectroscopic examination. All compounds are yellow in color with energy gaps commencing at 2.25 eV for **I**, 2.33 eV for **II**, 2.26 eV for **III**, and 2.67 eV for **IV** (Figure 4). Since these are molecular complexes, it is less meaningful to talk about band gaps; rather it is very likely that the energy gap arises from "localized" energy levels and can be assigned to S → M charge-transfer transitions.

Infrared spectra for **I** and **IV** are shown in Figure 5. **I** shows frequencies at 426 (m-s), 413 (m), and 384 (m) cm^{-1}

(17) (a) Axtell, E. A.; Kanatzidis M. G. *Chem. Mater.* **1996**, *8*, 1350. (b) Axtell, E. A.; Kanatzidis M. G. *Chem.—Eur. J.* **1998**, *4*, 2435. (c) Axtell, E. A.; Liao, J.-H.; Pikramenou, Z.; Kanatzidis M. G. *Chem.—Eur. J.* **1996**, *2*, 656. (d) Greenwood, N. N.; Earnshaw, A. *Chemistry of the elements*; Elsevier Science: New York, 1997.
(18) Coste, S.; Kopnin, E.; Evain, M.; Jobic, S.; Payen, C.; Brec, R. *J. Solid State Chem.* **2001**, *162*, 195.
(19) Chondroudis, K.; Kanatzidis, M. G. *Inorg. Chem.* **1998**, *37*, 3792.
(20) Hess, R.; Gordon, P. L.; Tait, D. C.; Abney, K. D.; Dorhout, P. K. *J. Am. Chem. Soc.* **2002**, *124*, 1327.
(21) McCarthy, T. J.; Kanatzidis, M.G. *J. Alloys Compd.* **1996**, *236*, 70.

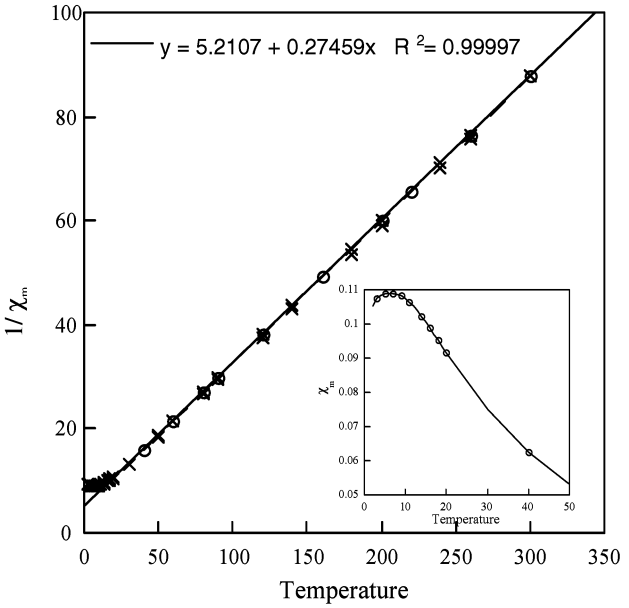

Figure 6. Plot of inverse molar susceptibility against temperature for $K_8[Mn_2(AsS_4)_4]$ showing a nearly Curie−Weiss behavior until 20 K. The inset shows a plot of molar susceptibility against temperature from 0 to 50 K. The susceptibility reaches a maximum at 6 K.

which can be assigned to As−S stretching. These frequencies are analogous to those observed in the clusters of $[Pt_3(AsS_4)_3]^{3-}$ and other reports.[22] There are several weak peaks below 300 cm^{-1}, which are contributed by Mn−S stretching modes. **IV** displays peaks at 468 (s), 431, 411, 385, 362, and 243 cm^{-1}. The peaks at 431, 411, and 385 cm^{-1} are due to As−S stretching while peaks below that are due to Cd−S vibrations. The peak at 468 cm^{-1} is attributed to S−S stretching.

Magnetism. $K_8[Mn_2(AsS_4)_4]$ is paramagnetic, nearly obeying the Curie−Weiss law over the temperature range 20−300 K. Figure 6 shows the plot of the reciprocal molar susceptibility ($1/\chi_m$) against temperature. The estimated μ_{eff} value of 5.4 μ_B confirms the Mn^{2+} nature of the metal even though it is slightly lower than the ideal 5.9 calculated for high-spin Mn^{2+} ions. The inset shows the dependence of χ_m in the range 0−50 K. As seen in the figure, the susceptibility shows a maximum indicating antiferromagnetic coupling. The maximum is observed at ∼6 K with a small Weiss constant, $\Theta \sim -19$ K, suggesting that the antiferromagnetic interactions are weak in nature, and this is in accordance with the long intracore Mn−Mn distance of 4.070(1) Å.

(22) (a) Chou, J. H.; Kanatzidis, M. G. *Inorg. Chem.* **1994**, *33*, 5372. (b) Siebert, H. *Z. Anorg. Allg. Chem.* **1954**, *225*, 275. (c) Nakamoto, K. *Infrared and Raman Spectra of Inorganic and Coordination Compounds*, 5th ed.; John Wiley & Sons: New York, 1997.

Concluding Remarks

Discrete molecules such as the anionic clusters $[Mn_2(AsS_4)_4]^{8-}$ and $[Cd(AsS_4)_2(AsS_5)_2]^{8-}$ form under essentially solution conditions inside a molten flux and crystallize as their alkali metal salts. Such outcomes in metal reactivity stress the utility of a flux approach in preparing not only complex solid-state compounds but, in many cases, also phases with discrete molecular species. The high negative charge of these clusters would have made it more difficult for them to be obtained via conventional solution techniques. The alkali metal thioarsenate flux is as interesting as its thiophosphate counterpart in exploring complex chalcogenides, and further investigation is called for to realize the full potential of these fluxes.

Acknowledgment. Financial support from the National Science Foundation (Grant DMR 0127644) is gratefully acknowledged.

Supporting Information Available: Tables of crystallographic details, atomic coordinates, isotropic and anisotropic displacement parameters for all atoms, and interatomic distances and angles for $K_8Mn_2As_4S_{16}$, $Rb_8Mn_2As_4S_{16}$, $Cs_8Mn_2As_4S_{16}$, and $Rb_8Cd_2As_4S_{18}$, in CIF format. This material is available free of charge via the Internet at http://pubs.acs.org.

IC049905U